Contents list available at CBIORE journal website

International Journal of Renewable Energy Development

Journal homepage: https://ijred.cbiore.id

Research Article

Comparative study on the quality and drying kinetics of temulawak by open-sun drying and biomass pyrolysis-integrated flat-bed dryer

Rosdanelli Hasibuan[a]*, Juliza Hidayati[b], Muhammad Khuwailid[a], Thiodorus Marvin Tjandra[a], Viqry Pramananda[a]

[a]*Department of Chemical Engineering, Faculty of Engineering, Universitas Sumatera Utara, Indonesia*

[b]*Department of Industrial Engineering, Faculty of Engineering, Universitas Sumatera Utara, Indonesia*

Abstract. Temulawak is a medicinal plant which is known for its active compound, curcumin. To extend its shelf life, freshly harvested rhizomes are typically subjected to drying to reduce their moisture content. However, the drying process must be carefully controlled to prevent curcumin degradation which is thermolabile. Despite its continued popularity for agricultural commodities drying because it requires minimal equipment and no operational expenses, open-sun drying (OSD) leaves the product vulnerable to external hazards such as dust, environmental pollutants, and ultraviolet exposure. A more suitable alternative is the flat-bed dryer (FBD) system. This study presents a comparison between OSD and an FBD integrated with a pyrolysis reactor for the drying of temulawak. The results demonstrated that the FBD significantly shortened the drying duration to 705 min at 70°C and 1.0 cm-thickness, compared with 2,490 min for OSD at the same thickness. The drying rate in the FBD reached 49.40–56.00 g/m^2.min, substantially higher than OSD (14.60–16.00 g/m^2.min). Curcumin content increased in both drying methods as a consequence of moisture reduction, with the FBD achieving 14.82 ppm within a markedly shorter drying time than OSD. Morphological analysis revealed cell-wall shrinkage and deformation of starch granules after drying, particularly in FBD-dried temulawak. Elemental composition analysis showed a considerable increase in mineral fractions after drying, corresponding to the reduction in moisture content. Drying kinetic modelling indicated that the Hasibuan–Daud model provided the best fit for FBD data, whereas the Midilli model offered the closest agreement with the experimental data obtained from OSD. The effective moisture diffusivity obtained for the FBD was 4.970 × 10^{-8} m^2/s, significantly higher than that of OSD, with an activation energy of 29.53 kJ/mol. Overall, the use of an FBD integrated with a pyrolysis reactor offers a sustainable and efficient alternative for the high-quality drying of medicinal plants, outperforming conventional OSD.

Keywords: Curcumin, Drying, Drying Kinetics, Flat-Bed Dryer, Temulawak

Received: 25th Nov 2025; Revised: 15th April 2026; Accepted: 7th May 2026; Available online: 16th May 2026

1. Introduction

Curcuma xanthorrhiza Roxb., commonly referred to as Javanese turmeric or temulawak, has gained prominence as a widely utilized medicinal species. Its cultivation is concentrated in Indonesia and several other Southeast Asian countries, such as Malaysia, Thailand, Vietnam, and the Philippines. Throughout its natural distribution regions, temulawak has long been used to treat a variety of illnesses and as a crucial component of jamu, a traditional Indonesian herbal medication. Temulawak's various pharmacological properties, such as its anti-inflammatory, antibacterial, and antioxidant effects have been linked to its medicinal potential. According to scientific research, temulawak's main phytochemical components include terpenoids and curcuminoids, which are thought to be principally in charge of its therapeutic qualities. The rhizome, which contains high concentrations of sesquiterpenoids and curcuminoids, serves as the principal medicinal part of the plant. Consequently, the market demand for temulawak rhizomes has been steadily increasing over time (Rahmat *et al.*, 2021).

One of the methods that can be applied to extend the postharvest shelf life of temulawak is drying. Traditionally, drying has served as a key preservation method by lowering the moisture content of agricultural products to levels that prolong their shelf life (Yahya *et al.*, 2023). This method uses hot air to lower water activity and moisture content to safe levels, preventing chemical, microbiological, and biochemical deterioration and allowing for longer storage times (Suherman *et al.*, 2025). Additionally, drying significantly decreases the product's mass and volume, resulting in reduced costs associated with storage, packaging, and transportation. In short, drying plays a vital role in food preservation, particularly in rural regions of developing countries where access to resources and infrastructure is limited (Susanto *et al.*, 2025).

For many generations, open-sun drying (OSD) has been the preferred crop drying method, particularly in developing nations. The amount of sunlight, the surrounding temperature, and the humidity affect the drying process in OSD, which can result in varying drying times (Sinuhaji *et al.*, 2025). Vegetables, fruits, grains, cereals, tobacco, and other materials have all been dried using OSD. The materials in OSD are laid out on the

* Corresponding author
Email: rosdanelli@usu.ac.id (R. Hasibuan)

https://doi.org/10.61435/ijred.2026.62014
ISSN: 2252-4940/© 2026.The Author(s). Published by CBIORE

ground and repeatedly flipped until they are thoroughly dry. Rain and clouds, insect and pest infestation, high dust levels, air pollution, and rodent and animal infiltration are some of the drawbacks of OSD. Additionally, the unpredictable drying process results in either excessive or insufficient drying, which degrades the product's quality (Mishra *et al.*, 2017). In addition, exposure to ultraviolet (UV) radiation from direct sunlight can damage agricultural materials and diminish their nutritional quality, ultimately reducing their hygienic safety. Although mechanical and microwave drying technologies offer efficient drying performance, their high operational costs and technical requirements limit their adoption, particularly among small-scale producers (Mahajan *et al.*, 2024). Nevertheless, OSD remains a preferred method, especially among farmers in developing countries. Undeniably, OSD is chosen due to the abundant availability of solar energy, its simple process, and low operational costs (Yahya *et al.*, 2022).

To address this issue, agricultural products such as temulawak can be dried using a flat-bed dryer (FBD) at both laboratory and pilot scales. The FBD is a type of mechanical dryer known for its simple design and ease of operation. It can be constructed using readily available and cost-effective materials. Typically, the drying chamber floor is made of fine wire mesh, a suitable supporting structure, or perforated metal sheets. The heating of air is commonly powered by petrol or diesel engines (Syariffuddeen *et al.*, 2020). During operation, warmed air is driven through a stationary bed of material by a blower, enabling efficient heat and mass transfer (Hung *et al.*, 2019). For instance, Ghiasi *et al.* (2016) utilized an FBD to produce commercially acceptable quality rice. Dried-rice by using FBD was found to have less physical damage and more uniform quality. Wincy *et al.* (2021) highlighted FBD benefits, showing that a reversible-airflow FBD coupled with a biomass gasifier performed more effectively than traditional biomass-fired dryers, making it suitable for large-scale rice drying. In the case of medicinal plant drying, Hasibuan *et al.* (2025) have reported the succesful of pyrolysis reactor-integrated FBD for red ginger drying. With a final moisture content of 9.71%, the study demonstrated that using FBD can yield the best dried product that fulfills the National Indonesian Standard (SNI) for red ginger.

However, the application of high temperatures during the drying of herbal plants can harm their distictive active components. Heat exposure can degrade active compounds, which can lower the dried product's quality (Hanief *et al.*, 2019; Yahya *et al.*, 2021). Therefore, the drying of herbal plants requires strict control of drying conditions to ensure low moisture content while preserving the active constituents as much as possible.

Beyond the need to carefully regulate drying conditions, ensuring a reliable energy source remains a significant obstacle in agricultural drying processes. Drying operations are known to consume substantial amounts of energy, representing roughly 7% to 15% of industrial energy use in many developing countries. At the same time, the food and agriculture sector relies heavily on fossil-based energy—approximately 68% of its total consumption—while contributing nearly 20% of global greenhouse gas emissions. With fossil fuel prices continuing to escalate, the exploration and adoption of renewable and alternative energy options have become increasingly critical (Susanto *et al.*, 2025). Therefore, the operation of drying equipment powered by renewable energy has emerged as a practical and sustainable solution.

One potential renewable energy source is energy derived from biomass. Using biomass as an energy source for drying has a number of advantages, including lower emissions, sustainable and renewable properties, affordability, and accessibility (Hasibuan *et al.*, 2025). During biomass pyrolysis, solid charcoal, bio-oil, and non-condensable gas are produced. Furthermore, heat is generated, which is usually wasted. This heat contains energy that can be utilized in the drying process of herbal plants, which generally does not occur at high temperatures. Integration of drying equipment with biomass-based energy, which is generated from pyrolysis or gasification, have been done for medicinal plants and spices drying, such as red ginger (Hasibuan *et al.*, 2025), Coriander (Gohain & Dutta, 2024), and small cardamon (Shreelavaniya *et al.*, 2021). Moreover, the use of a pyrolysis reactor is viewed as a cleaner alternative to the direct combustion of biomass. Through thermal decomposition under limited oxygen conditions, pyrolysis reduces atmospheric emissions while generating valuable by-products. In comparison, burning biomass in the presence of oxygen leads to complete oxidation, producing ash as well as smoke and harmful pollutants that negatively impact the environment (Hasibuan *et al.*, 2025).

In conjunction with this, an extensive study of the drying processes of sliced temulawak utilizing OSD and FBD combined with a pyrolysis reactor was carried out. In OSD, the drying process was carried out by adjusting the temulawak thickness. While in FBD, the drying air temperature and temulawak thickness were adjusted. Drying air in FBD was heated by the energy produced from the biomass pyrolysis reaction. The drying behavior, in term of moisture curve and drying rate, was observed. The quality of the dried temulawak was assessed via curcumin content, morphology, and elemental composition. Finally, drying kinetics modeling, moisture effective diffusivity calculations, and activation energy estimation were carried out. To the best of our knowledge, this kind of investigation is entirely novel in this study and has never been done previously.

2. Materials and Method

2.1 Drying Equipment Description

The temulawak originated from marketplaces in Medan City. The FBD, as shown in Figure 1, consists of a pyrolysis chamber and a drying chamber. The drying chamber is made up of three flat-beds, a ventilation system at the top, and a hot air channel at the bottom. The pyrolysis reactor (d = 80 cm, h = 120 cm) is made of stainless steel. This reactor is used for the pyrolysis of biomass (coconut shells) to produce charcoal and bio-oil. The pyrolysis process utilizes energy supplied by Liquefied Petroleum Gas (LPG). During pyrolysis, the energy from LPG decomposes the lignocellulosic components of the biomass. In addition to producing charcoal and liquid smoke, this process also releases heat that warms the air in the space between the pyrolysis chamber and the outer shell of the reactor (the area indicated as number 4 in Figure 1). This heated air is then transferred into the drying chamber using a blower (Krisbow® Electric Blower IRB6, 220 V, 600 W, 50 Hz, rotation speed 0–16,000 rpm, Indonesia). This drying system is designed to reutilize the heat that would otherwise be released into the ambient air during pyrolysis and convert it into useful energy to increase the drying air temperature. This approach also helps protect operators from direct exposure to the heat generated during the pyrolysis process. Other equipment used includes an oven (Memmert, Germany), electrical balance (Superior Mini Digital Platformscale, China), hygrometer (Mini LCD digital thermometer hygrometer, China), and anemometer (Krisbow KW06-562, Indonesia) were other pieces of equipment.

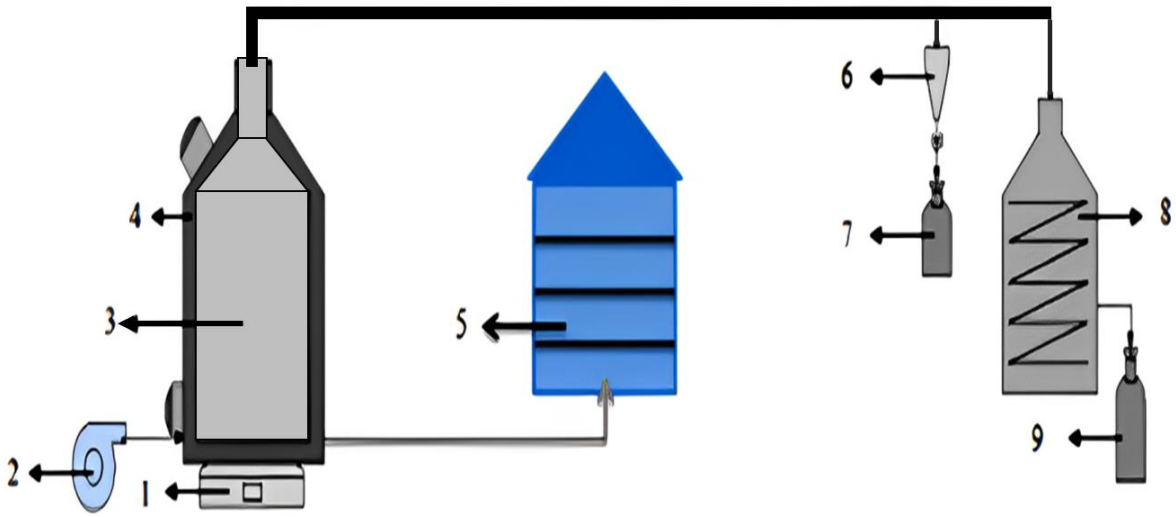

Fig. 1. The schematic of pyrolysis reactor-integrated flat-bed dryer
Note: (1) Burner; (2) Blower; (3) Pyrolysis chamber; (4) Empty space for hot air; (5) Drying chamber; (6) Trap; (7) Tar collecting tank; (8) Condenser; (9) Liquid smoke collecting tank

2.2 Drying of Temulawak

Temulawak was cleaned, allowed to air dry to eliminate any leftover water, and then sliced into 0.5 cm, 1.0 cm, and 1.5 cm thick slices. These slices were placed on two square-tray (10 x 10 cm). For OSD, the mass of both trays was measured every five minutes during the first two hours and then every hour after that. While in FBD, the measurement of mass tray was performed every five minutes. Drying was stopped when the constant mass was obtained (noted as equilibrium mass). Afterward, the temulawak were oven-dried at 105°C for 24 hours and then weighed to obtain their final mass. The mean mass was subsequently used to calculate the moisture ratio and drying rate. In the FBD experiments, drying was conducted at flat-bed positions located at 20 cm from the hot air inlet, with temperatures of 50°C, 60°C, and 70°C.

2.3 Drying Behavior

An analysis of the drying behavior of temulawak was carried out using the average mass and drying time data for each interval. These data were used for building the moisture ratio vs. drying time and drying rate vs. drying time graphs. Equations 1 through 3 were used to calculate the moisture content, moisture ratio, and drying rate.

$$MC_d = \frac{Wt - W_d}{W_d} \times 100\% \quad (1)$$

$$MR = \frac{MC_t - MC_e}{MC_0 - MC_e} \quad (2)$$

$$DR = \frac{\Delta w}{A \times \Delta t} \quad (3)$$

Where, w is sample mass (g), MC_d refers to moisture content in dry basis (%), MR refers to moisture ratio (dimensionless), DR is drying rate ($g/m^2.min$), and A is tray area (m^2). Subscript d, t, e, 0 refer to dry basis, certain time, equilibrium, an initial, respectively.

2.4 Curcumin Content Analysis

The curcumin content of all temulawak was quantified using a UV-visible spectrophotometer (Shimadzu, Model UV-1800, Serial No. A11635406115, Japan). The extraction process was performed by macerating the material in 96% ethanol (Technical grade, 96%, purchased from CV. Rudang Jaya, Medan, Indonesia) for 24 hours, employing a solid-to-solvent ratio of 1:10 (m/v). The resulting filtrate was separated from the solid residue using filter paper, concentrated to reduce the solvent volume, and analyzed using a UV-Visible spectrophotometer. Standard curcumin solutions (Merck, 94%, purchased from CV. Teknosains Indonesa) were prepared at concentrations of 1, 2, 3, 4, and 5 ppm, and their absorbances were measured. These absorbance values were used to develop a regression equation correlating absorbance with curcumin concentration. In addition, curcumin content analysis was performed on fresh temulawak to evaluate the changes in curcumin levels caused by the drying process.

2.5 Temulawak Characterization

The dried temulawak with the highest curcumin content was characterized, including morphological and elemental composition using Scanning Electron Microscope-Energy Dispersive X-ray (SEM-EDX, SEM-JEOL JCM-7000, Japan). For comparison, characterization was also performed on fresh temulawak to evaluate the effects of drying on its characteristics.

2.6 Drying Kinetic Modelling

To gain insight into the temulawak drying process, drying kinetic modeling was carried out based on OSD and FBD performances. The sample with the highest curcumin content was used for modeling purposes. Using Python software, the Midilli, Henderson-Pabis, Page, and Hasibuan-Daud models were used for establishing the drying kinetic model, as summarized in Table 1. MR stands for moisture ratio, t for drying time (min), and a, n, and m are constants.

2.7 Effective Moisture Diffusivity and Activation Energy (Ea)

The moisture diffusivity mechanism is governed by diffusion laws, as described by Fick's second law of diffusion (Equation 4).

Table 1
Drying Kinetic Models

Models	Equations	Ref
Midilli	$MR = a \exp(-kt^n) + bt$	(Midilli *et al.*, 2002)
Henderson-Pabis	$MR = a \exp(-kt)$	(Ertekin & Firat, 2015)
Page	$MR = \exp(-kt^n)$	(Ertekin & Firat, 2015)
Hasibuan-Daud	$MR = 1 - at^n \exp(-kt^m)$	(Hasibuan & Daud, 2007)

$$MR = \frac{8}{\pi^2} \sum_{n=0}^{\infty} \frac{1}{(2n+1)^2} \exp\left(-\frac{\pi^2 (2n+1)^2}{4L^2} D_{eff}\, t\right) \quad (4)$$

The simplification procedure of Equation (4) follows the steps reported by Raaf *et al.* (2024). The higher-order term in Equation (4), $(2n + 1)^2$, can be neglected, and n parameter can be assumed to be 0. Thus, Equation (4) can be rewritten as Equation (5) as follows.

$$MR = \frac{8}{\pi^2} \cdot \left(\frac{\pi^2}{4L^2} D_{eff}\right) t \quad (5)$$

Subsequently, Equation (5) can be linearized to obtain Equation (6). Through this equation, the effective moisture diffusivity (D_{eff}) is determined as the slope ($\frac{\pi^2}{4L^2} D_{eff}$) of the curve of ln MR vs. drying time.

$$\ln MR = \ln \frac{8}{\pi^2} - \left(\frac{\pi^2}{4L^2} D_{eff}\right) t \quad (6)$$

The obtained D_{eff} values were subsequently used to estimate the activation energy (Ea) of temulawak drying. In this case, the ln D_{eff} vs. $1/(T + 273.15)$ curve was developed, so that the slope was obtained as the value of (−Ea/R) based on Equation (7).

$$D_{eff} = D_0 \exp\left(-\frac{E_a}{RT}\right) \quad (7)$$

Where D_{eff} is the effective moisture diffusivity (m^2/s), D_0 is the pre-exponential factor (m^2/s), Ea is the activation energy (J/mol), R is the ideal gas constant (8.314 J/mol.K), and T is the drying temperature (K).

2.8 Statistical Analysis

Evaluating how well the kinetic models correspond to the experimental data is essential for identifying the best model in characterizing the drying behavior. To measure the adequacy of each model, four statistical indicators were applied, including coefficient of determination (R^2), Mean Square Error (MSE), Root Mean Square Error (RMSE), and the chi-square (χ^2). MSE reflects the mean value of the squared deviations between the observed data and the model predictions (Hasibuan *et al.*, 2023). RMSE quantifies the average distance between predicted and measured values, whereas R^2 indicates the extent to which the model outputs align with the actual experimental data (Kusuma *et al.*, 2023). Lastly, χ^2 represents the mean square of the deviations between the experimental data and the estimated values based on the mathematical model (Surendhar *et al.*, 2019). The best kinetic model was chosen based on the highest R^2 as well as the lowest MSE, RMSE, and χ^2 (Hasibuan *et al.*, 2023; Selvakumarasamy *et al.*, 2024; Surendhar *et al.*, 2019).

3. Results and Discussion

3.1 Temperature Profile of Drying Air

As shown in Figure 1, the pyrolysis reactor consists of two parts, namely the pyrolysis chamber (coded as number 3) and the empty space between the pyrolysis chamber and the outer reactor shell (coded as number 4). During the process, coconut shells in the pyrolysis chamber undergo thermal decomposition, producing biochar, pyrolysis vapor, and non-condensable gases. The biochar remains inside the pyrolysis chamber, while the pyrolysis vapor and non-condensable gases are directed to the condenser. The heat generated from the thermal decomposition of coconut shells increases the air temperature in the empty space between the pyrolysis chamber and the outer shell. This heated air is used as the drying medium and supplied to the drying chamber. Therefore, no mixing occurs between the pyrolysis vapor and non-condensable gases with the hot air used as the drying medium, ensuring that temulawak is free from exposure to harmful chemicals during the drying process.

The air temperature profiles of the from the pyrolysis reactor and at the drying chamber are shown in Figure 2. Initially, the air temperature from the reactor was set at 70°C when entering the drying chamber. Once the air entered the drying chamber, it was distributed throughout the chamber and contacted the flat-bed where temulawak was dried. This distribution resulted in a decrease in the drying air temperature to the range of 49.2–59.0°C. Interestingly, the relative humidity (RH) of the air both from the reactor and inside the drying chamber was successfully maintained at 10%. This is one of the advantages of the FBD, as it is capable of maintaining controlled drying conditions such as RH.

3.2 Drying Behavior of Temulawak

Drying behavior can be described through the moisture ratio curve, as shown in Figure 3. The moisture ratio represents the

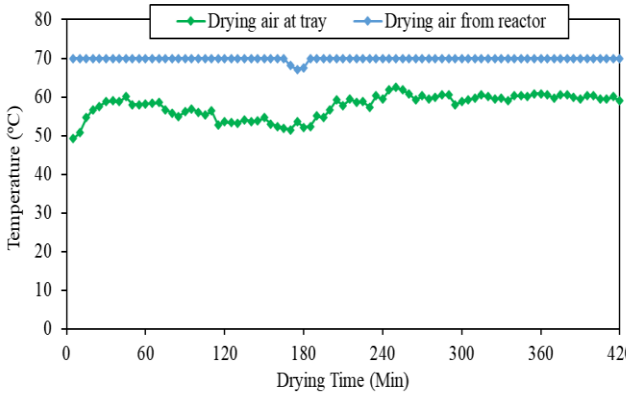

Fig. 2. Temperature profile of drying air in FBD

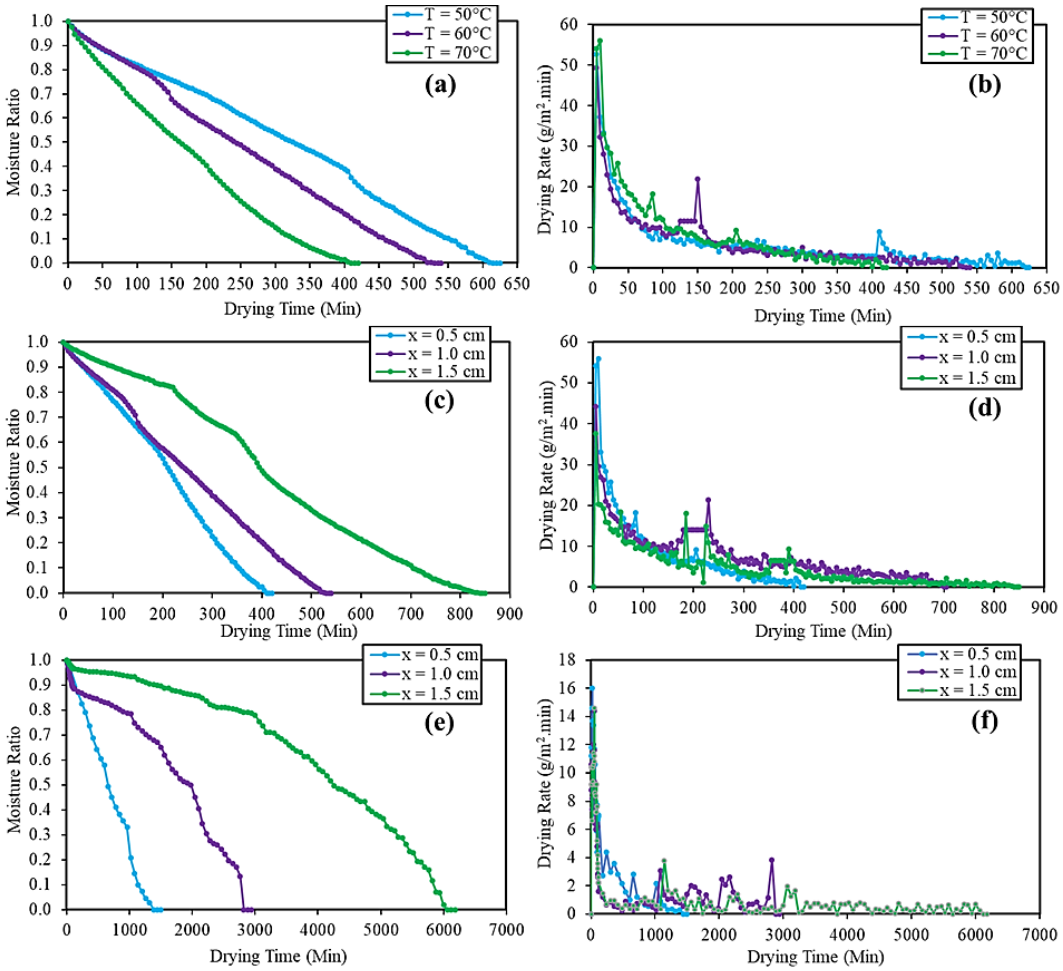

Fig. 3. Drying profiles of temulawak: (a) Moisture ratio in FBD at various temperature; (b) Drying rate in FBD at various temperature; (c) Moisture ratio in FBD at material thickness variation; (d) Drying rate in FBD at material thickness variation; (e) Moisture ratio in OSD at material thickness variation; (f) Drying rate in OSD at material thickness variation

proportion of remaining water in the material relative to its initial moisture content (Seremet (Ceclu) *et al.*, 2016). Previous studies have widely employed moisture ratio profiles to describe the drying behavior of various natural materials. Examples include their application in hot-air oven drying of ambarella (Ee *et al.*, 2021), infrared drying of pepper (Arslan *et al.*, 2021), and the dehumidification drying of moringa leaves (Siqhny *et al.*, 2024).

Figure 3a shows that elevating the drying temperature substantially accelerates the removal of moisture. The duration needed to reach a steady moisture ratio decreased to 625 minutes at 50°C, 540 minutes at 60°C, and 420 minutes at 70°C. Temperature serves as a key operating factor that strongly affects drying performance, product quality, and the overall drying kinetics. As the temperature increases, the drying process proceeds more rapidly while still allowing the material to retain acceptable quality (Sinuhaji *et al.*, 2025). The use of higher temperatures increases the rate of heat transfer, as elevated temperatures result in a greater vapor pressure deficit. Consequently, the moisture ratio decreases more rapidly, thereby shortening the required drying time (Wicaksono *et al.*, 2024). As drying progresses, the heated air supplies thermal energy to the material's surface, prompting the moisture present on the exterior to vaporize and diffuse into the surrounding air. This evaporation becomes faster when the drying temperature increases, when the air possesses lower humidity, or when these conditions occur simultaneously (Sasongko *et al.*, 2021). The continuous reduction of the moisture ratio suggests that the diffusion mechanism controls the internal mass transfer (Ambawat *et al.*, 2022). The drying time of temulawak in this study (420 minutes), obtained at a temperature of 70°C and a thickness of 0.5 cm, was shorter than that of oven drying under the same conditions, which required 500 minutes (Rangkuti *et al.*, 2024), and also shorter than drying using a double plate collector solar dryer, which required 540 minutes (Marnoto *et al.*, 2012). This result highlights the superiority of the flat-bed dryer (FBD) integrated with a pyrolysis reactor, which is capable of achieving faster drying compared to conventional drying systems.

It is clear from Figure 3c that thinner slices attain a constant moisture ratio faster. For thicknesses of 0.5 cm, 1.0 cm, and 1.5 cm, it took 420 minutes, 705 minutes, and 850 minutes, respectively, to achieve a constant moisture ratio at a drying temperature of 70°C. In contrast, it took 1500 minutes, 2940 minutes, and 6180 minutes to reach the same point using the OSD approach (Figure 3e). Diffusion of moisture into the air is hindered by thicker materials because they make it harder for moisture to move from the interior of the material to its surface. (Rangkuti *et al.*, 2024).

The drying of temulawak using both methods starts with a high drying rate, as seen in Figures 3b, 3d, and 3f. This results from the high initial moisture level, which evaporates more

readily. The drying rate progressively falls as drying goes on until it reaches a steady level. The observed trend indicates that the material's residual moisture content decreases with increasing drying time, making subsequent evaporation more challenging (Hasibuan *et al.*, 2025). In FBD with various drying temperatures (Figure 3b), the observed maximum drying rate ranged from 49.40 to 56.00 g/m^2.min. When the slice thickness was varied (Figure 3d), the maximum drying rate ranged from 37.60 to 54.10 g/m^2.min. In contrast, the OSD method resulted in a maximum drying rate of 14.60 to 16.00 g/m^2.min (Figure 3f). These differences are attributed to the distinct temperature conditions during the drying process. In FBD, the drying temperature is maintained constant with a relative humidity about 10%, whereas OSD produces a fluctuating temperature and humidity profile (T = 29.0-43.7°C, RH = 37–83%). Overall, the findings of this study confirm that the use of drying equipment can significantly shorten drying time.

3.3 Quality of Dried Temulawak

3.3.1 Curcumin Content

Figure 4 presents the curcumin content in temulawak before and after the drying process. The curcumin standard curve (Figure 4a) illustrates the correlation model between absorbance and curcumin concentration, with an R^2 value of 0.9891. This model was used to determine the curcumin content in temulawak before and after drying, as shown in Figures 3b to 3d. This approach was selected due to its simplicity and relatively lower instrumentation cost compared to more advanced techniques such as HPLC. Initially, fresh temulawak contained 12.41 ppm of curcumin. After drying, the curcumin content increased in both the FBD and OSD methods. This increase is primarily attributed to the moisture content reduction, which leads to a higher relative content of curcumin in the dried material.

Furthermore, in the FBD mode (Figure 4b), an increase in air temperature enhances the amount of moisture released from temulawak to the environment, resulting in a lower residual moisture content in the material. Consequently, the proportion of curcumin relative to the total compounds in temulawak dried at 60°C and 70°C becomes higher, leading to a slightly higher final curcumin content compared to temulawak dried at 50°C. A higher quality of temulawak resulting from drying at higher temperatures was also stated by Ramdhani *et al.* (Ramdhani *et al.*, 2021). In their report, the curcumin content of temulawak dried in an oven at 50°C was 417.75 mg, whereas that dried at 30°C contained 112.721 mg of curcumin.

On the other hand, the curcumin content in the FBD-dried temulawak appears to be lower than in the OSD mode. It is indicating the curcumin degradation caused by exposure to higher temperatures, although this effect is not very significant. This assumption is supported by the findings of Chen *et al.* (2014), who reported that the thermal degradation of curcumin begins at temperatures above 190°C. Masih & Iqbal (2022) also reported similar results, in which curcumin degradation above 190°C produced several toxic compounds, such as 1,4-dimethoxy-2-methylbenzene and 4-(4-hydroxy-3-methoxyphenyl)but-3-en-2-one. Therefore, it can be concluded that although curcumin is thermolabile, the drying processes applied in this study were still able to preserve the presence of curcumin in temulawak, both in the FBD and OSD modes.

Process parameters (drying temperature and material thickness), both in FBD and OSD, were found to have no significant effect on curcumin content. Although the OSD produced the highest curcumin concentration (15.16 ppm, Figure 4d), it required a prolonged drying time, up to 2,940 minutes (total drying time of 49 hours, as discussed in the previous section). In contrast, the FBD required only 705 minutes (11.75 hours) to reach its highest curcumin concentration of 14.82 ppm (Figure 4c). Based on these considerations, it can be concluded that FBD is a more effective method for preserving and even enhancing the quality of temulawak in a significantly shorter drying time compared to OSD. Additionally, materials dried using the OSD are more susceptible to contamination from dust, dirt, insects, and

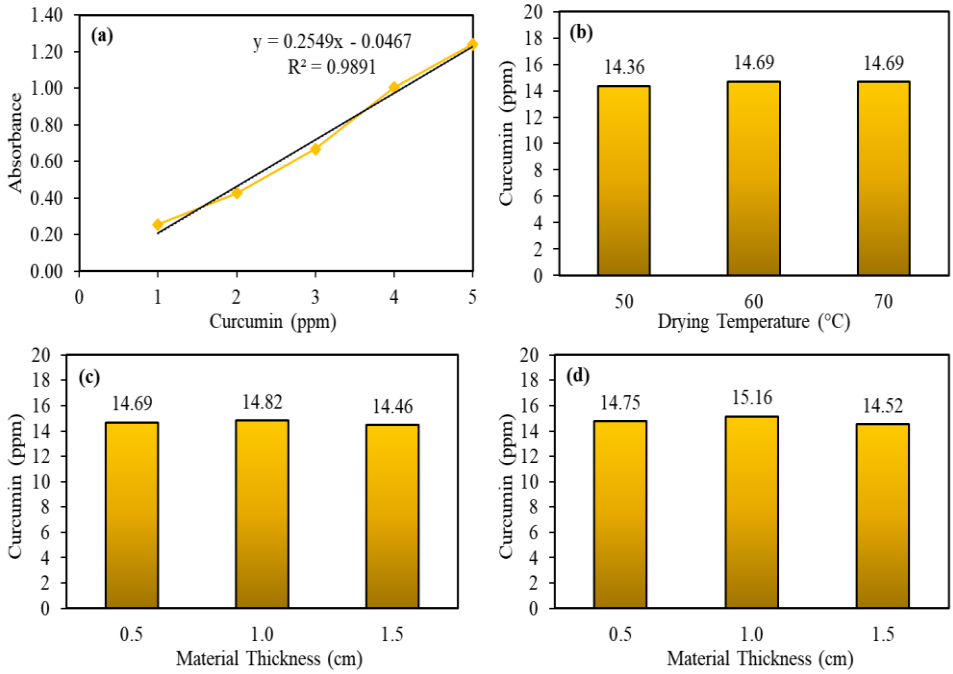

Fig. 4. Curcumin content in temulawak; (a) Curcumin standard curve; (b) curcumin content at various drying temperature in FBD; (c) curcumin content at various material thickness in FBD; (d) curcumin content at various material thickness in OSD

excessive ultraviolet (UV) exposure, which can degrade the quality of the dried product. Conversely, mechanical drying equipment such as FBD, not only cuts the drying time but also maintain product quality.

Based on the analysis results, there was a curcumin content difference of 0.34 ppm between the FBD and OSD. Nevertheless, the drying time required using FBD is much shorter than that of OSD. This means that drying by FBD can be completed within a single day, representing a clear advantage over OSD. Drying by FBD can be carried out anytime without dependence on weather conditions, as in OSD. In the long term, this advantage enables post-harvest processing of temulawak to be conducted efficiently without concerns regarding fluctuating weather conditions.

In the context of medicinal plants, drying is performed not only to reduce moisture content but also to preserve bioactive compounds from degradation. This is particularly important for herbal plants that contain various bioactive compounds with therapeutic potential, where the drying process must be carefully controlled to avoid reducing or damaging these active compounds. Based on our study, we highlight the reduction in moisture content, shorter drying time, and preservation of curcumin content during temulawak drying using FBD. These findings validate the potential of FBD to efficiently produce high-quality dried temulawak compared to conventional methods such as OSD.

Furthermore, the biomass pyrolysis process in generating heat also produces biochar and liquid smoke as a by-product. Numerous studies have reported the potential applications of liquid smoke in various fields, particularly in food preservation and energy. On the other side, bio-char can be utilized as energy sources, fertilizer, or adsorbent. The application of an FBD integrated with a pyrolysis reactor offers multiple advantages, including efficient drying, agricultural biomass management, and the production of value-added bio-char and liquid smoke. With further processing—which is beyond the scope of this study—the biochar and liquid smoke could be upgraded into high-quality products that may be sold by temulawak farmers as an additional income.

3.3.2 Morphology and Elemental Composition

The morphologies of temulawak before and after drying were examined using SEM, as shown in Figure 5. In this study, morphological observation was conducted on two dried temulawak with the highest curcumin content: (i) the sample dried at 70°C (1.0 cm) using FBD, and (ii) the sample dried using OSD (1.0 cm). Observation through SEM revealed that the fresh temulawak (Figure 5a) still exhibited a clearly defined cell wall structure. In addition, starch was visible on the surface of the fresh material with a diameter about 10 µm. After the drying process, a noticeable shrinkage of the cell wall structure was observed. This shrinkage was particularly evident in FBD-dried temulawak. Besides that, FBD-dried temulawak showed black zones, which correspond to the porosity formed during the drying process. In contrast, no black zones were observed in OSD-dried temulawak, indicating that no distinct porosity was formed after drying. The higher and relatively constant drying temperature in FBD promote to a greater removal of moisture content, resulting in more pronounced shrinkage of the temulawak cell structures. The formation of pores and microcracks facilitates internal moisture diffusion toward the surface, thereby reducing internal mass transfer resistance and contributing to the faster drying rates observed in the FBD mode. Furthermore, the starch granules in both FBD- and OSD-dried samples also exhibited a reduction in size, resulting granule diameters less than 10 µm. This reduction and shrinkage are attributed to the loss of moisture content in temulawak, including within the starch granules themselves, as a result of the drying process. Similar phenomena were reported by Abidin *et al.* (Abidin *et al.*, 2021) in the drying of several herbal plants, including temulawak, using a superabsorbent polymer-based dryer (Polydryer). The SEM images of dried temulawak revealed a more open microstructural morphology because the migration of moisture from the inner region to the outer region, leading to the rupture of the cellulosic walls of the starch granules.

The elemental composition of temulawak is presented in Figure 6. Both fresh and dried temulawak consist primarily of carbon and oxygen as the main components, along with a number of mineral. The total mineral content (elements other than C and O) in fresh temulawak was 6.72%. Minerals are commonly found in plants, including temulawak, such as K, Mn, P, Si, and other minerals (Manuhara *et al.*, 2022). After drying, the total mineral content increased to 15.39% in FBD-dried temulawak and 12.08% in OSD-dried temulawak. This change is attributed to the reduction in water fraction within the temulawak, which alters the relative proportion of the remaining minerals. This finding is evident from the decreased percentage of oxygen in temulawak after drying, indicating a reduction in moisture content. The increase of mineral content is mainly associated with the reduction of water content rather than chemical transformation or mineral loss. As a result of moisture removal during drying, trace minerals became detectable by EDX, while they were not detected in fresh temulawak prior to drying. By combining morphology observation and elemental identification, it can be concluded that drying primarily influence physical structure rather than elemental integrity. Drying does not introduce or create new elements, but affects

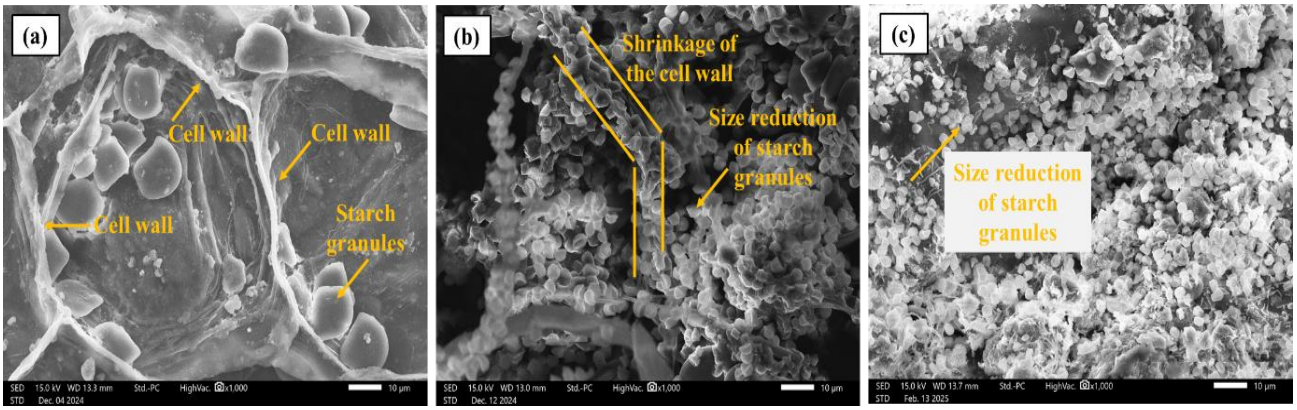

Fig. 5. Morphology of temulawak; (a) Before drying; (b) Dried by FBD at T = 70°C and x = 1.0 cm; (c) Dried by OSD at x = 1.0 cm

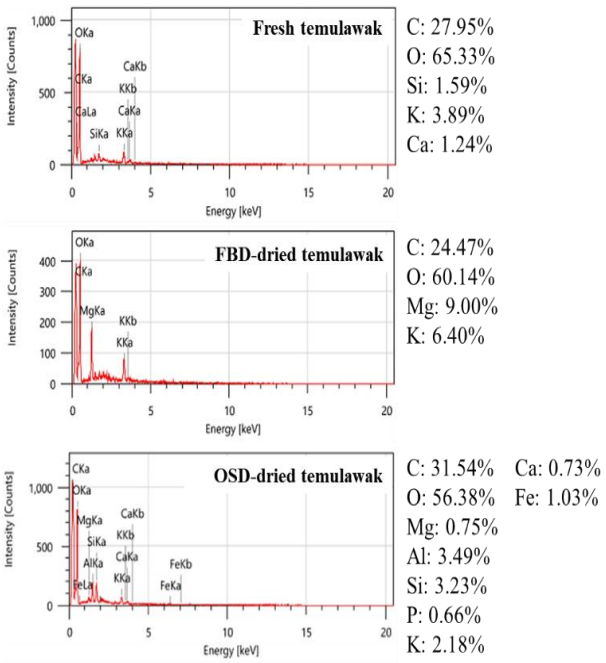

Fig. 6. Elemental composition of temulawak

their relative concentrations due to moisture removal. A similar observation was reported in our previous work using the same FBD equipment to dry red ginger slices, where potassium was detected (up to 7.05%) in the dried samples as a result of moisture loss (Hasibuan *et al.*, 2025). Furthermore, the total mineral content of FBD-dried temulawak was higher than OSD-dried samples, which can be attributed to the more intensive moisture removal achieved by the FBD. A similar trend was reported by previous studies. For instance, Özcan *et al.* (2005) reported higher mineral contents in oven-dried basil leaves than in OSD-dried samples. Anawar *et al.* (2011) report in the drying of *Lavandula luisieri* and *Cistus ladanifer*, where freeze-drying and oven-drying resulted in higher mineral concentrations compared to ambient-air drying.

An interesting aspect observed from the elemental analysis results is the diversity of mineral detected between FBD- and OSD-dried temulawak. Although the FBD-dried temulawak exhibited a higher total mineral content, the number of detected mineral types was lower (two minerals) compared to OSD-dried temulawak, in which seven mineral elements were identified. This phenomenon can be explained by differences in the moisture transport mechanisms during drying. FBD operates at a higher air temperature, constant relative humidity, and forced airflow, which accelerates the migration of water molecules from the core of the material to the surface and leading to more intensive microstructural shrinkage. As a result, some minerals become trapped within the contracted microstructure and do not reach the surface of the temulawak slices, rendering them undetectable by EDX analysis. In contrast, OSD involves a very small temperature gradient between the ambient air and the temulawak material, resulting in a much slower moisture transfer rate. Consequently, minerals have sufficient time to redistribute toward the microstructural surface of temulawak, allowing a greater variety of mineral elements to be detected by EDX. This difference in moisture transport rates is supported by the calculated effective moisture diffusivity values presented in Table 2, where the diffusivity coefficient for FBD was approximately 9.8 times higher than that of OSD. This explains why OSD-dried temulawak exhibited a greater diversity of detectable mineral elements compared to the FBD-dried samples. This finding is also consistent with the principle of elemental analysis using EDX, in which the elements present on the surface of a sample interact with the rays emitted by the EDX instrument (Taslim *et al.*, 2025).

Table 2
D_{eff} Values in Temulawak Drying

Drying Modes	Operating Conditions	D_{eff} (m^2/s)
FBD	T = 50°C, x = 0.5 cm	1.242×10^{-8}
	T = 60°C, x = 0.5 cm	1.648×10^{-8}
	T = 70°C, x = 0.5 cm	2.333×10^{-8}
	T = 70°C, x = 1.0 cm	4.970×10^{-8}
OSD	T = 29.0-43.7°C x = 1.0 cm	5.071×10^{-9}

3.4 Drying Kinetics

Direct measurement of several parameters during drying is often challenging, which is why mathematical modeling is employed to overcome these limitations. Such models enable the prediction of temperature profiles, moisture evolution, and even airflow behavior throughout the drying process. They also play a crucial role in dryer design, performance evaluation, and process optimization, all of which are important for maintaining product safety and quality (Suherman *et al.*, 2020). In the present study, the drying behavior of temulawak was analyzed using thin-layer drying models. The thin-layer concept assumes that the material forms a uniform layer exposed to controlled drying air conditions, both in temperature and relative humidity (Hasibuan *et al.*, 2023), and it is widely used for studying the drying patterns of many agricultural commodities (Raaf *et al.*, 2024). The Midilli, Henderson-Pabis, Page, and Hasibuan-Daud models are among the kinetic models utilized. The Hasibuan-Daud model is categorized as an empirical model, whereas Midilli, Henderson-Pabis, and Page are categorized as semi-theoretical (Ertekin & Firat, 2015). Semi-theoretical representing modifications of existing models through the addition of specific constants to overcome the limitations of earlier formulations (Raaf *et al.*, 2024). They act as bridges between basically theoretical and empirical models; they are frequently constructed by simplifying Fick's second rule of diffusion or improving earlier models (Hasibuan *et al.*, 2023). Conversely, empirical models do not depend on predefined assumptions about the drying mechanism; instead, they use regression-based relationships to link average moisture content with drying time (Taki *et al.*, 2025).

Figures 7 and 8 visualize the comparison of MR from experimental data and prediction from drying kinetic models, both from FBD and OSD, respectively. Meanwhile, Table 3 outlines the kinetic constants and the model's accuracy in forecasting the moisture ratio. Visually, the curves of the Midilli, Page, and Hasibuan–Daud models closely align—indeed, they overlap in the case of FBD—with the experimental data points. This is also supported by high coefficients of determination (R^2 > 0.98) for these models under FBD conditions. This finding provides an initial indication of the accuracy of the models in representing the moisture ratio profile during temulawak drying.

The occurrence of negative parameter values, – k and b in Midlli model, as well as m in Hasibuan-Daud model –, is

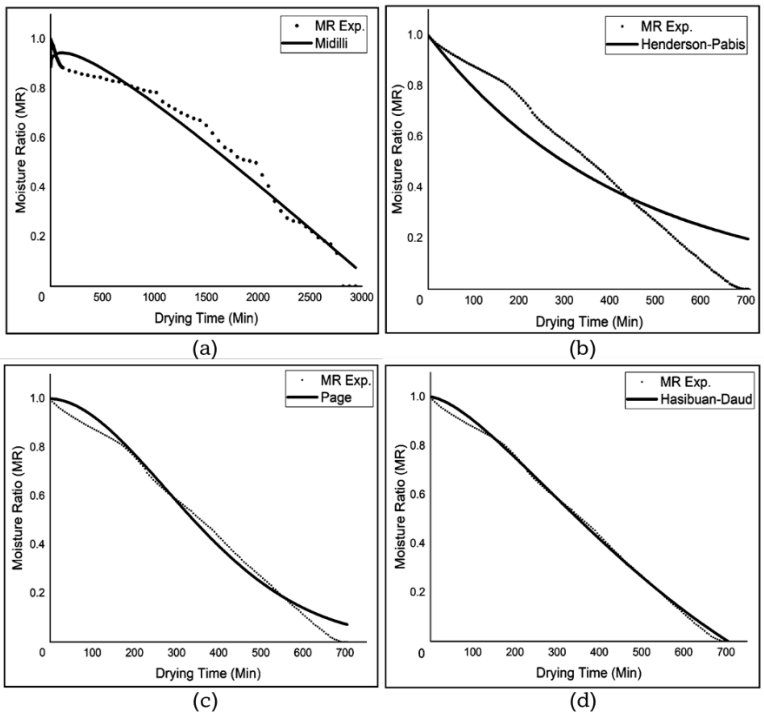

Fig. 7. Comparison of MR from experimental data and prediction for FBD-dried temulawak: (a) Midilli; (b) Henderson-Pabis; (c) Page; (d) Hasibuan-Daud

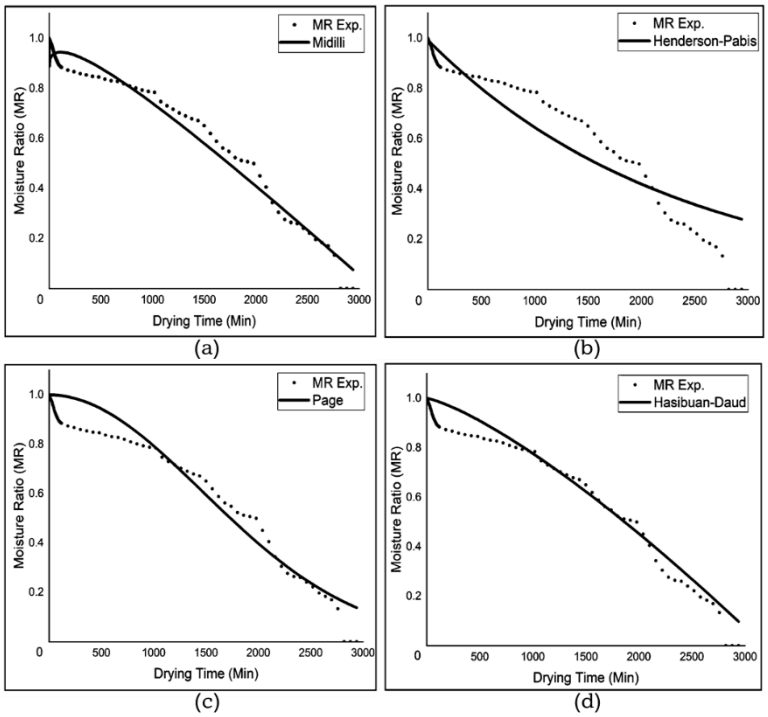

Fig. 8. Comparison of MR from experimental data and prediction for OSD-dried temulawak: (a) Midilli; (b) Henderson-Pabis; (c) Page; (d) Hasibuan-Daud

attributed to the nature of the unconstrained nonlinear regression procedure in this study. The optimization algorithm minimizes the global error between predicted and experimental MR without imposing physical restrictions on parameter signs. Consequently, certain parameters may adopt negative values as a mathematical compensation mechanism to reduce residual errors, particularly in the later stages of drying. From a physical standpoint, drying rate constants are expected to be positive. However, it is important to note that these thin-layer drying models (Midilli, Page, Henderson–Pabis, and Hasibuan–Daud) are semi-empirical and primarily intended for curve-fitting purposes rather than strict mechanistic interpretation. Therefore, the presence of negative coefficients does not necessarily invalidate the predictive capability of the model within the experimental range.

Table 3
Drying Kinetic Modelling

Kinetic Models	Parameters					R^2	MSE	RMSE	χ^2
	k	n	a	b	m				
FBD (T = 70°C, x = 1.0 cm)									
Midilli	0.000002	2.1397	0.9311	0.0000	-	0.99293	0.00073	0.00037	0.00013
Henderson-Pabis	0.0023	-	1.0000	-	-	0.94310	0.01011	0.00495	0.00787
Page	0.000015	1.8431	-	-	-	0.98796	0.00134	0.00067	0.00136
Hasibuan-Daud	0.0023	1.5852	0.0001	-	0.9095	0.99772	0.00027	0.00013	0.00012
OSD (x = 1.0 cm)									
Midilli	-0.0115	0.4960	0.8913	-0.0005	-	0.97064	0.00240	0.04895	0.00254
Henderson-Pabis	0.0004	-	0.9929	-	-	0.87731	0.01001	0.10005	0.01030
Page	0.000000251	1.9886	-	-	-	0.93679	0.00516	0.07181	0.00530
Hasibuan-Daud	0.0238	1.2897	0.00003	-	-0.0002	0.96303	0.00302	0.05492	0.00319

Although some predicted curves appear visually distant from experimental points at certain drying periods, particularly Henderson-Pabis model, the high R^2 values indicate that the models are capable of explaining most of the variability in the data. In drying studies, R^2 can remain high even when localized deviations occur, particularly because the moisture ratio decreases monotonically from values close to unity toward equilibrium. Thus, small systematic deviations may not significantly reduce the overall coefficient of determination.

The statistical analysis shows that the Hasibuan–Daud model demonstrates the best capacity to describe the experimental data for FBD, whereas the Midilli model is the most accurate model for OSD. This is indicated by the highest R^2 values as well as the lowest MSE, RMSE, and χ^2 values for the Hasibuan–Daud model in the FBD mode and the Midilli model in the OSD mode. The Hasibuan-Daud model accounts for both periods of increasing and decreasing drying rates. The Midilli model, on the other hand, describes the material's moisture ratio as a function of drying time and is composed of an exponential and a linear term (Ertekin & Firat, 2015). Multiple investigations confirmed that the Hasibuan-Daud Model is appropriate for explaining the drying behavior of agricultural commodities, including Persian shallot slices (Taki *et al.*, 2025), lime (Somjai *et al.*, 2023), banana (Mugundan *et al.*, 2021), and pineapple (López-Cerino *et al.*, 2019). Furthermore, Midilli model has a flexible structure with several adjustable parameters, allowing it to accommodate various forms of complex drying curves (Sinuhaji *et al.*, 2025).

3.5 Effective Moisture Diffusivity and Activation Energy

The effective moisture diffusivity (D_{eff}) is a critical transport property in drying process modelling of fruits and vegetables. D_{eff} is a function of temperature and moisture content. For fruits and vegetables, D_{eff} ranges from 10^{-12} to 10^{-6} m^2/s (Onwude *et al.*, 2016). In the present work, D_{eff} for dried temulawak—notably the samples with the highest curcumin content—was determined using an approach based on Fick's second law. This formulation provides a direct means of associating moisture diffusivity with the drying rate, particularly during the falling-rate period where internal mass transfer dominates (Chen *et al.*, 2020).

Table 2 summarizes the D_{eff} values for temulawak dried with OSD and FBD. The D_{eff} values for temulawak under FBD mode were higher than those under OSD mode, as was to be predicted. This is because FBD uses a higher and more consistent temperature, which improves the transfer of moisture in temulawak. A similar phenomenon was reported by Olawoye *et al.* (2017) who stated that the D_{eff} values of hot air-dried banana were higher than OSD-dried banana. In other investigation, Raaf *et al.* (2022), who investigated D_{eff} in amla fruit drying using oven drying and OSD, also reported that the D_{eff} values under oven drying were higher than those under OSD. In addition, an increase in drying temperature also increased the D_{eff}, from 1.242×10^{-8} to 2.333×10^{-8} m^2/s. Higher drying temperatures can speed up the flow of water molecules, reducing the material's moisture content more quickly. Consequently, the D_{eff} value becomes higher (Thuwapanichayanan *et al.*, 2011).

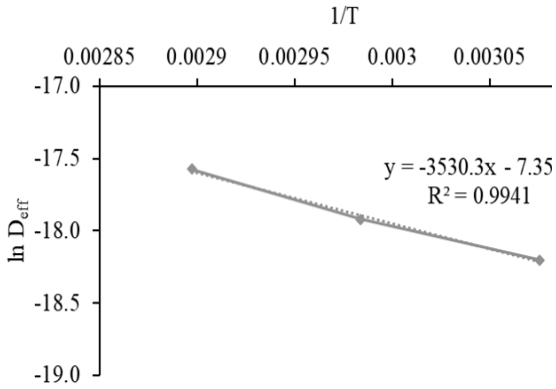

Fig. 9. 1/T vs. ln D_{eff} curve

The D_{eff} data at various drying temperatures were subsequently used to estimate the activation energy (Ea) of temulawak drying. The determination of Ea was carried out using the Arrhenius equation that relates D_{eff} to the drying temperature (Hasibuan & Bairuni, 2018). Because it requires a range of drying temperature data, the estimation of Ea could only be performed for temulawak drying using an FBD. Figure 9 shows the plot of ln D_{eff} vs. 1/T, where the slope of this graph is −3530.3 with an R^2 value of 0.9941. Using this slope, the Ea of temulawak drying was obtained as 29.53 kJ/mol. It is interesting to note that, to the best of the information we have, no prior research has examined the D_{eff} and Ea during temulawak drying. The D_{eff} and Ea values of temulawak, especially when dried utilizing an FBD coupled with a pyrolysis reactor, are thus presented for the first time in this study.

4. Conclusion

The drying efficacy of temulawak slices utilizing OSD and FBD combined with a biomass pyrolysis reactor was thoroughly compared in this study. Material thickness for OSD, as well as drying temperature and material thickness for FBD, were

methodically varied. The outcomes showed that using FBD resulted in the highest-quality dried temulawak while preserving its curcumin content. Compared to 49 hours with OSD, the drying time was drastically shortened to 11.75 hours. Thinner slices and higher drying temperatures sped up the drying process in FBD. The drying rate profiles from both systems showed a similar pattern, starting at an increasing drying rate and progressively decreasing until they reached a steady state. The highest drying rate was observed in the FBD system, attributed to the maintained drying conditions (temperature and humidity). The maximum drying rate ranged 49.40-56.00 g/m^2.min for FBD at various temperatures and 37.60-54.10 g/m^2.min at various slices thickness. In contrast, the maximum drying rate in OSD around 14.60-16.00 g/m^2.min. SEM procedures showed that the dried temulawak, especially using the FBD method, had altered starch granules and shrunk cell walls. The Hasibuan-Daud model showed the best fit to the experimental data for FBD, while Midilli became the most advantageous model for OSD.

Moreover, the FBD system yielded higher effective moisture diffusivity coefficients compared to OSD. Overall, this study highlights the advantages of FBD integrated with biomass pyrolysis reactor in drying and preserving the quality of temulawak slices, both in terms of drying efficiency and product quality. Future studies are recommended to include exergy analysis, techno-economic evaluation, and environmental impact assessment to further validate the FBD system as an appropriate and sustainable drying technology.

Acknowledgments

The authors gratefully acknowledge the Research Institute of Universitas Sumatera Utara (LP-USU) for providing financial support for this work, through the TALENTA research grant, scheme of Development Research-Technology Readiness Level of 6-7, fiscal year 2024 (Contract number: 18589/UN5.1.R/PPM/2024, dated 30th May 2024).

Author Contributions: R.H.: supervision; conceptualization; investigation; funding acquisition; writing—review and editing; J.H.: project administration; M.K.: data curation; T.M.J.: data curation; V.P.: Writing—original draft preparation; data analysis; visualization. All authors have read and agreed to the published version of the manuscript.

Funding: This study received financial support from the Research Institute of Universitas Sumatera Utara (LP-USU) through the TALENTA Research Grant, under the TALENTA research grant, scheme of Development Research-Technology Readiness Level of 6-7, for the 2024 fiscal year.

Conflicts of Interest: The authors declare no conflict of interest.

References

Abidin, A. Z., Putra, R. P., Izzati, A. U. N., & Christian, Y. (2021). Design and Performance Evaluation of a Superabsorbent Polymer-Based Dryer for Medicinal Plants. *Journal of Food Processing and Preservation*, *45*, 1–10. https://doi.org/10.1111/jfpp.15988

Ambawat, S., Sharma, A., & Saini, R. K. (2022). Mathematical Modeling of Thin Layer Drying Kinetics and Moisture Diffusivity Study of Pretreated Moringa oleifera Leaves Using Fluidized Bed Dryer. *Processes*, *10*(2464), 1–24. https://doi.org/10.3390/pr10112464

Anawar, H. M., Canha, N., Freitas, M. C., Regina, I. S., & Garcia-Sanchez, A. (2011). Effects of Different Drying Processes on the Concentrations of Metals and Metalloids in Plant Materials. *Journal of Radioanalytical and Nuclear Chemistry*, *289*, 29–34. https://doi.org/10.1007/s10967-011-1051-9

Arslan, A., Soysal, Y., & Keskin, M. (2021). Infrared Drying Kinetics and Color Qualities of Organic and Conventional Sweet Red Peppers. *Journal of Tekirdag Agricultural Faculty*, *18*(2), 260–272. https://doi.org/10.33462/jotaf.750623

Chen, C., Venkitasamy, C., Zhang, W., Khir, R., Upadhyaya, S., & Pan, Z. (2020). Effective Moisture Diffusivity and Drying Simulation of Walnuts under Hot Air. *International Journal of Heat and Mass Transfer*, *150*, 1–10. https://doi.org/10.1016/j.ijheatmasstransfer.2019.119283

Chen, Z., Xia, Y., Liao, S., Huang, Y., Li, Y., He, Y., Tong, Z., & Li, B. (2014). Thermal Degradation Kinetics Study of Curcumin with Nonlinear Methods. *Food Chemistry*, *155*, 81–86. https://doi.org/10.1016/j.foodchem.2014.01.034

Ee, C. T., Khaw, Y. J., Hii, C. L., Chiang, C. L., & Djaeni, M. (2021). Drying Kinetics and Modelling of Convective Drying of Kedondong Fruit. *ASEAN Journal of Chemical Engineering*, *21*(1), 93–103. https://doi.org/10.22146/ajche.62932

Ertekin, C., & Firat, M. Z. (2015). A Comprehensive Review of Thin-Layer Drying Models Used in Agricultural Products. *Critical Reviews in Food Science and Nutrition*. https://doi.org/10.1080/10408398.2014.910493

Ghiasi, M., Ibrahim, M. N., Kadir Basha, R., & Abdul Talib, R. (2016). Energy Usage and Drying Capacity of Flat-Bed and Inclined-Bed Dryers for Rough Rice Drying. *International Food Research Journal*, *23*, S23–S29. https://www.cabidigitallibrary.org/doi/pdf/10.5555/20173175929

Gohain, R. J. B., & Dutta, P. P. (2024). Solar Biomass Hybrid Drying and Quality Evaluation of Eryngium foetidum in an Innovative Newly Developed Solar Dryer. *Solar Energy*, *270*, 1–14. https://doi.org/10.1016/j.solener.2024.112416

Hanief, S., Pane, Y. M., & Hasibuan, R. (2019). The Effect of The Molecular Sieve Position on The Efficiency of Solar-Molecular Sieve Combination Dryer. *AIP Conference Proceedings*, *2085*, 1–8. https://doi.org/10.1063/1.5095050

Hasibuan, R., & Bairuni, M. (2018). Mathematical Modeling of Drying Kinetics of Ginger Slices. *AIP Conference Proceedings*, *1977*, 1–8. https://doi.org/10.1063/1.5042903

Hasibuan, R., & Daud, W. R. W. (2007). Through Drying Characteristics of Oil Palm Empty Fruit Bunch (EFB) Fibers Using Superheated Steam. *Asia-Pacific Journal of Chemical Engineering*, *2*, 35–40. https://doi.org/10.1002/apj.053

Hasibuan, R., Haryanto, B., Nafsun, A. I. binti, Pramananda, V., Siregar, F. F., & Fazillah, R. (2025). Drying of Red Ginger Slices Using Tray Dryer Integrated with Pyrolysis Reactor as a Heat Source: Evaluation on the Drying Characteristics, Red Ginger Quality, and Drying Kinetics. *Case Studies in Chemical and Environmental Engineering*, *11*, 1–11. https://doi.org/10.1016/j.cscee.2024.101055

Hasibuan, R., Sari, W. N., Manurung, R., & Alexander, V. (2023). Drying Kinetic Models of Rice Applying Fluidized Bed Dryer. *Mathematical Modelling of Engineering Problems*, *10*(1), 334–339. https://doi.org/10.18280/mmep.100138

Hung, N. Van, Martinez, R., Tuan, T. Van, & Gummert, M. (2019). Development and Verification of a Simulation Model for Paddy Drying with Different Flatbed Dryers. *Plant Production Science*, *22*(1), 119–130. https://doi.org/10.1080/1343943X.2018.1518723

Kusuma, H. S., Izzah, D. N., & Linggajati, I. W. L. (2023). Microwave-Assisted Drying of Ocimum sanctum Leaves: Analysis of Moisture Content, Drying Kinetic Model, and Techno-Economics. *Applied Food Research*, *3*, 1–22. https://doi.org/10.1016/j.afres.2023.100337

López-Cerino, I., López Cruz, I. L., Janjai, S., Nagle, M., Mahayothee, B., & Müller, J. (2019). Mathematical Modelling of the Thin Layer Drying of Pineapple (Ananas comosus, L.): Experiment at Village-Scale in a Greenhouse Type Solar Dryer. *Ingeniería Investigación y Tecnología*, *20*(2), 1–10. https://doi.org/10.22201/fi.25940732e.2019.20n2.016

Mahajan, K. M., Patil, V. H., & Koli, T. A. (2024). Design Analysis of an

Innovative Solar Biomass Hybrid Dryer for Drying Turmeric. *Interactions*, *245*(145), 1–28. https://doi.org/10.1007/s10751-024-01965-3

Manuhara, Y. S. W., Sugiharto, S., Kristanti, A. N., Aminah, N. S., Wibowo, A. T., Wardana, A. P., Putro, Y. K., & Sugiarso, D. (2022). Antioxidant Activities, Total Phenol, Flavonoid, and Mineral Content in the Rhizome of Various Indonesian Herbal Plants. *Rasayan Journal of Chemistry*, *15*(4), 2724–2730. https://doi.org/10.31788/RJC.2022.1548024

Marnoto, T., Mahreni, Nuri, W., Ardinanto, B., & Puspitasari, R. E. (2012). Drying of Curcuma (Curcuma xanthorrhiza roxb) Using Double Plate Collector Solar Dryer. *Proceeding of International Conference on Chemical and Material Engineering 2012*, 1–5.

Masih, R., & Iqbal, M. S. (2022). Thermal Degradation Kinetics and Pyrolysis GC–MS Study of Curcumin. *Food Chemistry*, *385*, 1–7. https://doi.org/10.1016/j.foodchem.2022.132638

Midilli, A., Kucuk, H., & Yapar, Z. (2002). A New Model for Single-Layer Drying. *Drying Technology*, *20*(7), 1503–1513. https://doi.org/10.1081/DRT-120005864

Mishra, M. K., Shrestha, K. R., Sagar, V., & Amatya, R. K. (2017). Performance of Hybrid Solar-Biomass Dryer. *Nepal Journal of Environmental Science*, *5*, 61–69. https://doi.org/10.3126/njes.v5i0.22717

Mugundan, C. A., Sheeba, K. N., & Sureshkumar, P. (2021). *Modelling and Performance Studies of Solar Dryer for Processed Banana*. https://doi.org/10.13052/rp-9788770227896

O¨zcan, M., Arslan, D., & U¨nver, A. (2005). Effect of Drying Methods on the Mineral Content of Basil (Ocimum basilicum L.). *Journal of Food Engineering*, *69*, 375–379. https://doi.org/10.1016/j.jfoodeng.2004.08.030

Olawoye, B. T., Kadiri, O., & Babalola, T. R. (2017). Modelling of Thin-Layer Drying Characteristic of Unripe Cardaba banana (Musa ABB) Slices. *Cogent Food and Agriculture*, *3*, 1–12. https://doi.org/10.1080/23311932.2017.1290013

Onwude, D. I., Hashim, N., Janius, R. B., Nawi, N. M., & Abdan, K. (2016). Modeling the Thin-Layer Drying of Fruits and Vegetables: A Review. *Comprehensive Reviews in Food Science and Food Safety*, *15*, 599–618. https://doi.org/10.1111/1541-4337.12196

Raaf, A., Mulana, F., Syamsuddin, Y., Suriaini, N., & Dani, M. (2024). Pemodelan Kinetika Pengeringan Buah Amla (Indian Gooseberry). *AGROINTEK: Jurnal Teknologi Industri Pertanian*, *18*(4), 861–870. https://doi.org/10.21107/agrointek.v18i4.19802

Raaf, A., Putra, T. W., Mulana, F., Syamsuddin, Y., & Supardan, M. D. (2022). Investigation of Kinetics of Amla (Emblica officinalis) Fruit Drying Process. *South African Journal of Chemical Engineering*, *41*, 10–16. https://doi.org/10.1016/j.sajce.2022.03.011

Rahmat, E., Lee, J., & Kang, Y. (2021). Javanese Turmeric (Curcuma xanthorrhiza Roxb.): Ethnobotany, Phytochemistry, Biotechnology, and Pharmacological Activities. *Evidence-Based Complementary and Alternative Medicine*, *2021*, 1–15. https://doi.org/10.1155/2021/9960813

Ramdhani, R. P., Sutanto, H., Puspita, D. M., & Puteri, M. D. P. T. G. (2021). Oven Drying and Water Extraction of Curcuma xanthorrhiza for Hygiene Improvement in the Production of Jamu Cekok, a Traditional Appetite Stimulant Herbal Medicine. *Journal of Functional Food and Nutraceutical*, *3*(1), 51–55. https://journal.sgu.ac.id/jffn/index.php/jffn/article/view/72

Rangkuti, M. T. A., Hasibuan, R., Haryanto, B., & Pramananda, V. (2024). The Effect of Drying Temperature and Material Thickness on the Drying Characteristics and Drying Kinetics of Curcuma Drying Using an Oven. *IOP Conference Series: Earth and Environmental Science*, *1352*, 1–11. https://doi.org/10.1088/1755-1315/1352/1/012087

Sasongko, S. B., Rini, B. P., Maehiroh, H., Utari, F. D., & Djaeni, M. (2021). The Effect of Temperature on Vermicelli Drying under Dehumidified Air. *IOP Conference Series: Materials Science and Engineering*, *1053*, 1–6. https://doi.org/10.1088/1757-899x/1053/1/012102

Selvakumarasamy, S., Kulathooran, R., & Rengaraju, B. (2024). Effect of Drying on Insulin Plant Leaves for Its Sustainability and Modeling the Drying Kinetics by Mathematical Models and Artificial Neural Network. *Environmental Modeling and Assessment*, *29*, 901–914. https://doi.org/10.1007/s10666-024-09974-w

Seremet (Ceclu), L., Botez, E., Nistor, O., Andronoiu, D. G., & Mocanu, G. (2016). Effect of Different Drying Methods on Moisture Ratio and Rehydration of Pumpkin Slices. *Food Chemistry*, *195*, 104–109. https://doi.org/10.1016/j.foodchem.2015.03.125

Shreelavaniya, R., Kamaraj, S., Subramanian, S., Pangayarselvi, R., Murali, S., & Bharani, A. (2021). Experimental Investigations on Drying Kinetics, Modeling and Quality Analysis of Small Cardamom (Elettaria cardamomum) Dried in Solar-Biomass Hybrid Dryer. *Solar Energy*, *227*, 635–644. https://doi.org/10.1016/j.solener.2021.09.016

Sinuhaji, T. R. F., Suherman, S., Hadiyanto, H., Ardan, A., & Rahmawati, S. (2025). Evaluation and Comparison of Drying Models in Open Sun Drying and Photovoltaic and LPG Burner Assisted Hybrid Solar Drying System. *Case Studies in Chemical and Environmental Engineering*, *11*, 1–15. https://doi.org/10.1016/j.cscee.2025.101104

Siqhny, Z. D., Sari, A. R., Utari, F. D., & Djaeni, M. (2024). Drying Kinetics and Thermal Energy Evaluation of Moringa oleifera leaves Drying Using Dehumidification with Zeolite. *Journal of Bioresources and Environmental Sciences*, *3*(1), 53–60. https://doi.org/10.61435/jbes.2024.19811

Somjai, T., Nuthong, P., & Wongsa, J. (2023). Thin-Layer Drying Kinetics and Quality Attributes of Osmotic Dehydrated Lime Slices. *Journal of Engineering Science and Technology*, *18*(4), 1957–1972. https://jestec.taylors.edu.my/Vol%2018%20Issue%204%20August%202023/18_4_10.pdf

Suherman, S., Asy-Syaqiq, M. A., Rahayu, E., Simanjuntak, Z., Sussardi, A. R., Hadiyanto, H., Prasetiyono, B. W. H. E., & Saptoro, A. (2025). Performance of a Mixed-Mode Air Recirculation Solar Dryer Integrated with Thermal Energy Storage and Evacuated Tube Solar Collector for Drying Sweet Corn Kernels. *Journal of Food Science and Technology*, *62*, 1260–1271. https://doi.org/10.1007/s13197-024-06090-1

Suherman, S., Widuri, H., Patricia, S., Susanto, E. E., & Sutrisna, R. J. (2020). Energy analysis of a hybrid solar dryer for drying coffee beans. *International Journal of Renewable Energy Development*, *9*(1), 131–139. https://doi.org/10.14710/ijred.9.1.131-139

Surendhar, A., Sivasubramanian, V., Deepanraj, B., & Vidhyeswari, D. (2019). Energy and Exergy Analysis, Drying kinetics, Modeling and Quality Parameters of Microwave-Dried Turmeric Slices. *Journal of Thermal Analysis and Calorimetry*, *136*, 185–197. https://doi.org/10.1007/s10973-018-7791-9

Susanto, E. E., Saptoro, A., Kumar, P., Tiong, A. N. T., Putranto, A., & Suherman, S. (2025). 7E + Q Analysis of a Novel Modified Mixed-Mode Solar Dryer for Porang Chips. *Drying Technology*, *43*(5), 858–877. https://doi.org/10.1080/07373937.2025.2473564

Syariffuddeen, M. A. A., Yahya, S., Ruwaida, A. W., Zainun, M. S., Shahrir, A., Azman, H., Shafie, A., Zaimi, Z. A. M., Hafiz, M. A. T. M., Redzuan, S. A., Aliq, J., Shukri, J., Faewati, A. K., Mohsin, Y., & Shanmugevelu, S. (2020). Evaluation on Drying Temperature of Grain Corn and Its Quality Using Flat-Bed Dryer. *ASM Science Journal*, *13*(4), 78–83. https://www.akademisains.gov.my/asmsj/article/evaluation-on-drying-temperature-of-grain-corn-and-its-quality-using-flat-bed-dryer/

Taki, M., Noshad, M., Jasemi, M. M., & Isvandi, F. (2025). Application of Even Span Greenhouse Solar Dryer (ESGSD) for Drying Persian Shallot; Kinetic Analysis, Machine Learning Modeling and Quality Evaluation. *Case Studies in Thermal Engineering*, *68*, 1–14. https://doi.org/10.1016/j.csite.2025.105880

Thuwapanichayanan, R., Prachayawarakorn, S., Kunwisawa, J., & Soponronnarit, S. (2011). Determination of Effective Moisture Diffusivity and Assessment of Quality Attributes of Banana Slices During Drying. *LWT Food Science and Technology*, *44*, 1502–1510. https://doi.org/10.1016/j.lwt.2011.01.003

Wicaksono, A. S., Hasibuan, R., & Tambun, R. (2024). Corn Drying with a Rotary Dryer: Effect of Airspeed and Drying Temperature Operating Conditions. *AIP Conference Proceedings*, *3026*, 1–6. https://doi.org/10.1063/5.0202658

Wincy, W. B., Edwin, M., & Sekhar, S. J. (2021). Exergetic Evaluation of

a Biomass Gasifier Operated Reversible Flatbed Dryer for Paddy Drying in Parboiling Process. *Biomass Conversion and Biorefinery*, *13*, 4033–4045. https://doi.org/10.1007/s13399-021-01322-2

Yahya, M., Fahmi, H., & Hasibuan, R. (2022). Experimental Performance Analysis of a Pilot-Scale Biomass-Assisted Recirculating Mixed-Flow Dryer for Drying Paddy. *International Journal of Food Science*, *2022*, 1–15. https://doi.org/10.1155/2022/4373292

Yahya, M., Fahmi, H., Hasibuan, R., & Fudholi, A. (2023). Development of Hybrid Solar-Assisted Heat Pump Dryer for Drying Paddy. *Case Studies in Thermal Engineering*, *45*, 1–13. https://doi.org/10.1016/j.csite.2023.102936

Yahya, M., Hasibuan, R., Sundari, R., & Sopian, K. (2021). Experimental Investigation of the Performance of a Solar Dryer Integrated with Solid Desiccant Coloums Using Water Based Solar Collector for Medicinal Herb. *International Journal of Power Electronics and Drive Systems*, *12*(2), 1024–1033. https://doi.org/10.11591/ijpeds.v12.i2.pp1024-1033